International Journal of ChemTech Research
CODEN(USA): IJCRGG ISSN : 0974-4290
Vol.5, No.4, pp 1694-1706, April-June 2013

Experimental And Theoretical Vibrational Spectra, Factor Group Analysis And Quantum Chemical Calculations Of Creatininium Benzoate

A. Jahubar Ali [1], S. Thangarasu[2], S. Athimoolam[3] and S. Asath Bahadur [2,*]

[1]Department of Science and Humanities, National College of Engineering, Maruthakulam, Tirunelveli 627 151, India.

[2]Department of Physics, Kalasalingam University, Krishnankoil 626 190, Tamilnadu, India

[3]Department of Physics, University College of Engineering Nagercoil, Anna University of Technology Tirunelveli, Nagercoil 629 004, Tamilnadu, India

***corres. author: s_a_bahadur@yahoo.co.in, Mobile No.: 99425 89442**

Abstract: A combined experimental and theoretical study on vibrational spectra of creatininium benzoate is employed. Theoretical studies were done by the Density Functional Theory (DFT) using the B3LYP function with the 6-311++G(d,p) basis set and established a theoretical molecular structure. The solid phase FT-IR and FT-Raman spectra of creatininium benzoate have been recorded in the range of 4000-400 cm^{-1}. The calculated wavenumbers were compared with the corresponding experimental values. A pronounced change was observed in the N–H stretching frequencies of the NH_2 group. It is observed that the amide NH_2 group is influenced by the intermolecular hydrogen bond in the crystal. Packing calculations were performed with the Gaussian 03W package program. Theoretically constructed spectra coincide satisfactorily with those of experimental spectra.

Key Words: Creatininium benzoate, FT-IR spectrum, FT-Raman spectrum, Factor group analysis, Vibrational analysis, DFT.

1. INTRODUCTION

Creatinine anhydride $C_4H_7N_3O$, a nitrogeneous organic acid, which is found in muscle tissue and blood. It is normally excreted in the urine as a metabolic waste. Urinary excretion of creatinine is relatively constant from day to day, and reflects mainly the amount of muscle tissue in the body. Therefore the amounts of various components of urine are often expressed relative to creatinine. It is mainly filtered by the kidney, though a small amount is actively secreted. There is little-to-no tubular reabsorption of creatinine. If the filtering of the kidney is deficient, creatinine levels rise. As a result, creatinine blood levels may be used to calculate creatinine clearance (ClCr), which reflects the Glomerular Filtration Rate (GFR). The GFR is clinically important because it is a measurement of renal function. Measurement of creatinine levels in serum and determination of renal clearance of creatinine are widely used for laboratory diagnosis of renal and muscular function [1].

Creatinine has three different tautomeric forms of similar energy and hydrogen bond donor–acceptor arrays require binding each of these forms [2]. NMR spectroscopic studies and high-level theoretical calculations indicate that the amino tautomer of creatinine is more stable in aqueous solutions [3, 4]. On the other hand, in the gas phase, the imino tautomer is probably more stable [2], while in a sufficiently acidic medium, creatinine is protonated apparently at N3, forming the creatininium cation with strong delocalized charge [5, 6]. Creatinine, being a natural metabolite of creatine, is an important bioligand. The presence of several donor groups in its main tautomeric forms determines its strong coordination capacity. The complexation ability towards a number of metal ions: Ag(I), Hg(II), Cd(II), Zn(II), Co(II), Ni(II), Cu(II), Pt(II), Pd(II) was studied [7-11].

Similarly studies of organic–inorganic hybrid materials, including amino acids and various inorganic acids [12-14] have received a great deal of attention in recent years because of their electrical, magnetic and optical properties [15]. Hydrogen bonds in hybrid compounds are of interest because of their widespread biological occurrence. For example, hydrogen bonds between phosphate groups and histidine imidazole groups are involved in the active-site substrate–binding mechanism of ribonucleases [16] and in regulation of the oxygen affinity of deoxy hemoglobin by 2,3, diphosphoglycreate [17]. In particular, N-H…O hydrogen bonds are predominant in determining the formation of secondary structure elements in proteins and base- pairing in nucleic acid and their biomolecular interactions. The crystal structure of creatinine with organic/inorganic acid complexes were already reported such as creatininium nitrate [18], creatininium benzoate [19] and Creatininium dipicolinate monohydrate [20] etc. The complexes were studied to understand the hydrogen bonding of creatinine with other acids, hence the stability and reactivity of the complexes. Based on the above specifics, in the present investigation, creatinine was treated with the benzoic acid and the title compound was crystallized.

The crystal structure of creatininium benzoate was reported by Bahadur et al [19]. It is observed from literature that neither quantum chemical calculations, nor the vibrational spectra of creatininium benzoate have been reported so far. Though, there are few reports for spectral analysis of creatininium and benzoate ions separately, there is not systematic study about this ionic crystalline ensemble. Therefore the present investigation was undertaken to study the vibrational spectra of this molecule completely and to identify the various modes with greater accuracy. The Density functional theory calculations have been performed to predict molecular structure of creatininium benzoate vibrational assignments and hydrogen bonding interactions.

2. EXPERIMENTAL

2.1. PREPARATION

Crystals of creatininium benzoate were crystallized from an aqueous solution of creatinine and benzoic acid with a stoichiometric ratio of 1:1 at low temperature by slow evaporation. After 10 days, needle-shaped, transparent and colorless crystals of creatininium benzoate were obtained.

2.2. SINGLE CRYSTAL XRD STUDIES

Unit cell parameters and structure of creatininium benzoate crystal were determined from single-crystal X-ray diffraction data obtained with a Bruker SMART APEX CCD area detector diffractometer (graphite-monochromated, MoK_α = 0.71073 Å).

Unit cell dimensions	a = 8.569(4) Å $\alpha = 90°$
	b = 6.236(3) Å $\beta = 99.68(1)°$
	c = 22.121(8) Å $\gamma = 90°$
Volume	V = 1165.23(6) $Å^3$

The above results are perfectly matches with the earlier results [19]. Hence, the crystalline phase is confirmed and the CIF of the creatinine benzoate [19] is used for DFT and other calculations.

2.3. VIBRATIONAL SPECTROSCOPIC MEASUREMENTS

Infrared spectral measurements were made with a Nexus 670 FTIR spectrometer with a resolution of ~1–2 cm^{-1} over the range 4000–400 cm^{-1}. The samples are being mixed with KBr powder and pressed into disc under high pressure. The disc was used to obtain the spectra. Radiation of 1064 nm from the Nexus 670 FT Raman spectrometer of Nd:YAG laser was used as the source of excitation. The laser power was maintained at 1.5 watts. The measured spectral lines had a resolution of 2–3 cm^{-1} in the same range of the wavenumber Indium-Gallium Arsenide detector is used as a detector. The experimental FT-IR and FT-Raman spectra of creatininium benzoate crystals are shown in Figs.1 and 2, respectively.

Fig. 1. FT-Infrared spectrum of creatininium benzoate

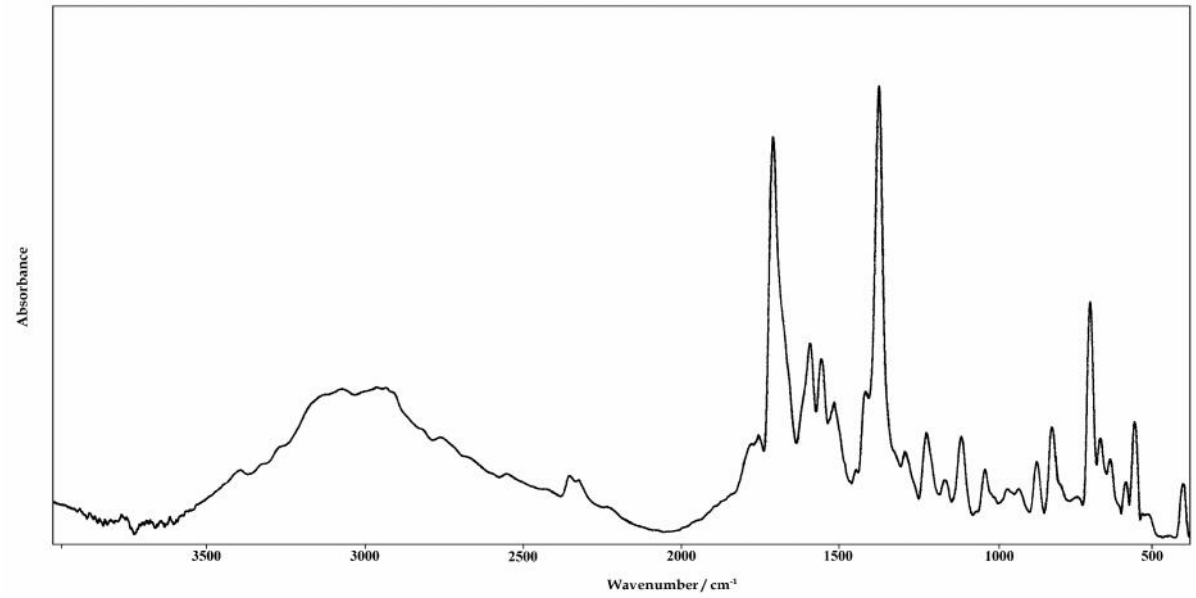

Fig. 2. FT-Raman spectrum of creatininium benzoate

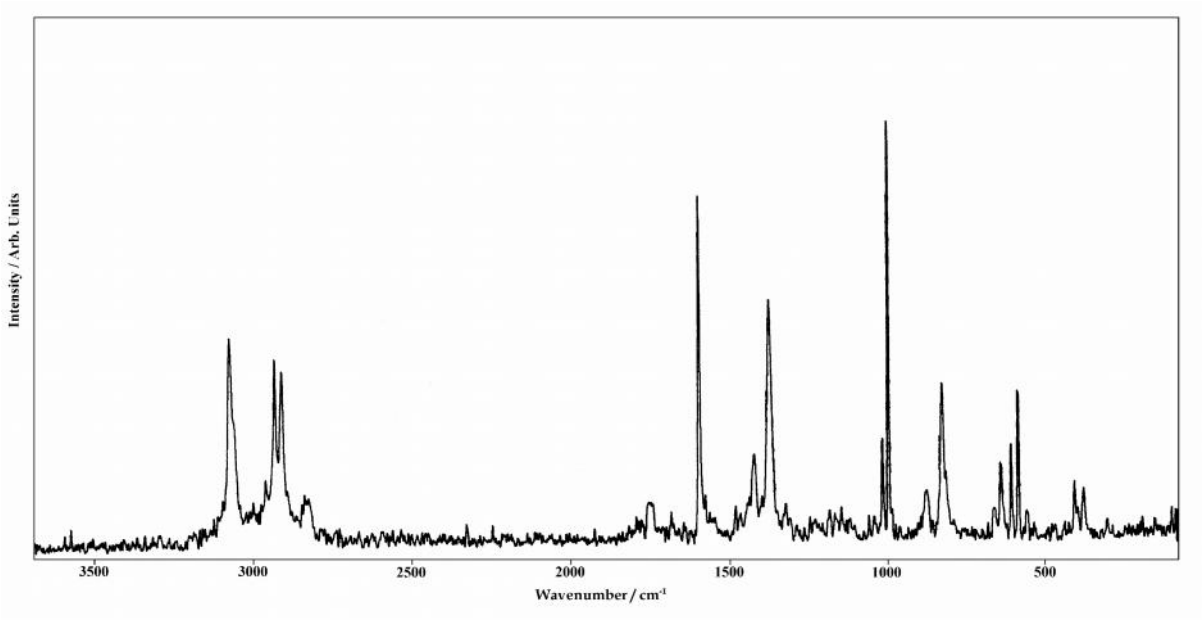

3. COMPUTATIONAL DETAILS

The entire theoretical calculations were performed by the B3LYP levels on a Pentium IV/3.02 GHz computer using Gaussian 03W [21] program package and gradient geometry optimization [22]. The first task for the computational work was to determine the optimized geometry of the compound. The spatial coordinate positions of creatininium benzoate, as obtained from an X-ray structural analysis [19], were used as the initial coordinates for the theoretical calculations. At B3LYP level, initial geometry was minimized without any constraint in the potential energy using the 6-311++G(d,p) basis set. The optimized structural parameters were used to calculate vibrational frequencies. Then vibrationally averaged nuclear positions of creatininium benzoate were used for harmonic vibrational frequency calculations resulting in IR and Raman frequencies. We have used the density functional theory [23] with the three-parameter hybrid function (B3) [24] for the exchange part and the Lee-Yang-Parr (LYP) correlation function [25], accepted as a cost-effective approach, for the computation of molecular structure and vibrational frequencies. Vibrational frequencies computed at DFT level have been adjudicated to be more reliable. Finally, the calculated normal mode vibrational frequencies provide thermodynamic properties also through the principle of statistical mechanics.

Vibrational frequency assignments were made with a high degree of accuracy, by combining the results of the GAUSSVIEW program [26] with symmetry considerations. Stimulated IR and Raman spectra of the title compound are shown in Figs. 3 and 4, respectively.

Fig. 3. IR spectrum of creatininium benzoate (Theory)

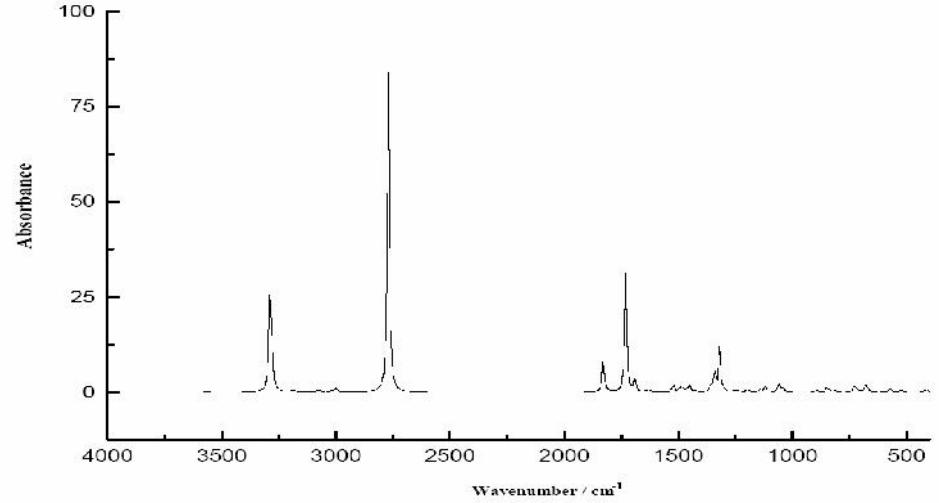

Fig. 4. Raman spectrum of creatininium benzoate (Theory)

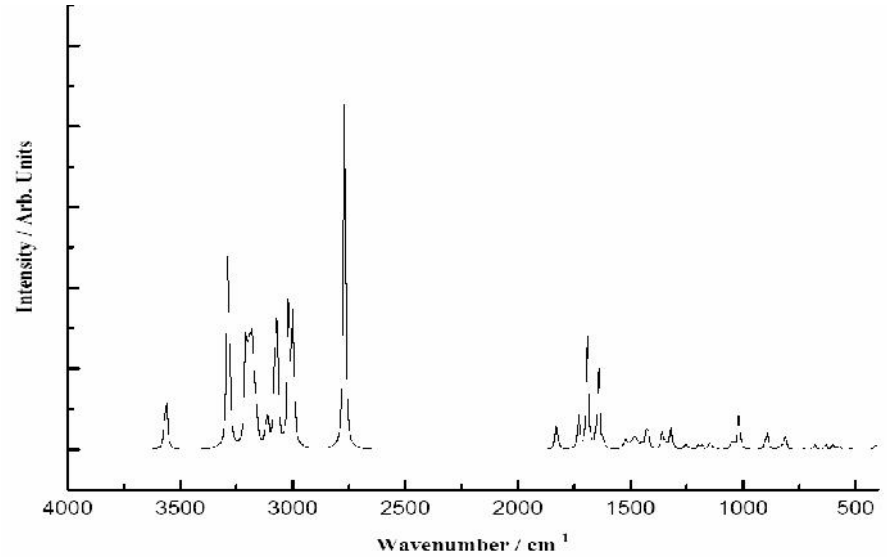

4 RESULTS AND DISCUSSION

4.1. MOLECULAR GEOMETRY

The X-ray structural analyses of creatininium benzoate [19] crystal shows that the structure is monoclinic space group $P2_1/c$ with Z = 4. The calculated geometrical parameters by **DFT/** ***B3LYP / 6-311++G(d,p)*** basis set are listed in Table 1 in accordance with the atom numbering scheme (Fig. 5). Table 1 compares the calculated bond lengths and angles for creatininium benzoate with those of experimentally available from X-ray structural data [19]. The optimized bond length of C—C in phenyl ring fall in the range from 1.391 Å to 1.400 Å for B3LYP/6-311++G(d,p) method, which are good agreement with those of experimentally reported values for C—C bond length of phenyl ring of this and similar molecules [27].

The structural investigation of the title compound reveals the protonation on the N site of the creatinine molecule and its cationic nature. The asymmetric unit of the tile compound contains one creatininium cation and one benzoate anion, with normal bond lengths and angles corresponding to those observed in similar structure [18]. The expected proton transfer from benzoic acid to creatinine occurs at N11 of the imidazolyl ring. This results increase in the C1—N11 bond distance [1.359 (2) Å] and a decrease of C1—N13 bond distance [1.311 (2) Å] compared with the corresponding values found in the neutral creatinine molecule 1.349 (2) and 1.320 (3) Å, respectively [28].

Initial geometry was taking from the X-ray data for DFT calculations. In general, biomolecules having the proton donor groups such as O—H and N—H can be involved in inter and intramolecular hydrogen bonds. The acceptor atoms are O and N as both behave as donor and acceptor. In the presence structure is observed that the N—H···O bond interaction in X-ray studies [19] was changed as O—H···N bond (Fig.5). From the theoretical values, it is observed that most of the optimized bond lengths are slightly larger than the experimental values. These two changes are due to the fact that the theoretical calculations have been carried out on isolated molecule in gaseous phase whereas the experimental results correspond to molecules in solid state [29]. The largest discrepancies between the calculated and experimental geometrical parameters are observed for C-N & C-O bonds. The strong deviation for these bonds may arise due to the hydrogen bonding interactions. The variations between experimental and calculated bond lengths are in the range of 0.02 to 0.12 Å. Whereas the bond angles from theoretical calculations are close to the experimental values (Table 1). The maximum difference is about 2.8°.

Fig. 5. The labeling of atoms in creatininium benzoate structure.

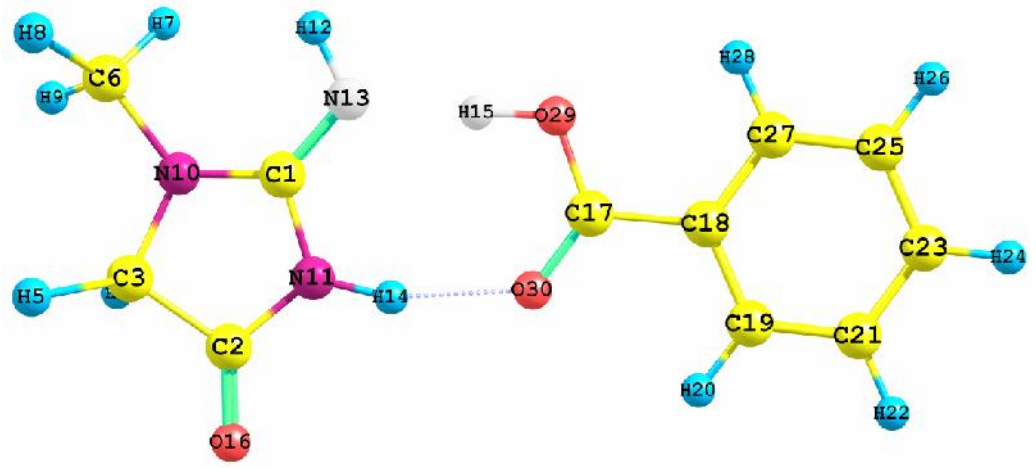

Table 1 Optimized geometrical parameters of creatininium benzoate
[Bond length (Å) and angle (°)]

Parameters	*B3LYP / 6-311++G(d,p)*	*Experimental[19] (creatininium benzoate)*
Bond length (Å)		
Creatininium cation		
N10—C1	1.373	1.321(2)
C1—N13	1.288	1.311(2)
C1—N11	1.388	1.359(2)
C2—O16	1.207	1.207(2)
C2—N11	1.375	1.373(2)
C2—C3	1.532	1.508(2)
C3—N10	1.456	1.449(2)
C3—H4	1.094	0.97
C3—H5	1.097	0.97
C6—N10	1.448	1.448(2)
C6—H7	1.092	0.96
C6—H8	1.098	0.96
C6—H9	1.091	0.96
N11—H14	1.030	0.93 (2)
N13—H12	1.014	0.89(2)
N13—H15		0.92(2)
Benzoate anion		
C17—O30	1.227	1.254(2)
C17—O29	1.321	1.259(1)
C17—C18	1.492	1.506(2)
C18—C27	1.400	1.381(2)
C18—C19	1.399	1.389(2)
C19—C21	1.391	1.375(2)
C19—H20	1.083	0.93
C21—C23	1.395	1.369(3)
C21—H22	1.084	0.93
C23—C25	1.395	1.376(3)
C23—H24	1.084	0.93
C25—C27	1.392	1.383(2)
C25—H26	1.084	0.93
C27—H28	1.082	0.93
Bond angle (°)		
Creatininium cation		
N13—C1—N10	130.3	127.5(1)
N13—C1—N11	122.2	121.5(1)
N10—C1—N11	107.7	110.9(1)
O16—C2—N11	127.9	126.4(1)
O16—C2—C3	126.8	127.8(1)
N11—C2—C3	105.4	105.8(1)
N10—C3—C2	103.1	102.8(1)
N10—C3—H4	112.6	111.2
C2—C3—H4	110.5	111.2
N10—C3—H5	112.6	111.2
C2—C3—H5	109.4	111.2
H4—C3—H5	108.6	109.1
N10—C6—H7	110.3	109.5

N10—C6—H8	112.5	109.5
H7—C6—H8	108.8	109.5
N10—C6—H9	109.0	109.5
H7—C6—H9	107.4	109.5
H8—C6—H9	108.7	109.5
C1—N10—C6	123.9	127.2(1)
C1—N10—C3	110.6	109.9(1)
C6—N10—C3	122.4	122.7(1)
C1—N11—C2	112.8	110.5(1)
C1—N11—H14	120.5	121.3(9)
C2—N11—H14	126.7	127.9(9)
C1—N13—H12	113.4	121.3(9)
C1—N13—H15		117.2(9)
H22—N13—H15		121.4(9)
Benzoate anion		
O30—C17—O29	123.8	124.2(1)
O30—C17—C18	122.0	116.7(1)
O29—C17—C18	114.2	119.1(1)
C27—C18—C19	119.8	118.5(1)
C27—C18—C17	121.6	121.8(1)
C19—C18—C17	118.7	119.7(1)
C21—C19—C18	120.1	121.1(1)
C21—C19—H20	121.2	119.4
C18—C19—H20	118.7	119.4
C23—C21—C19	120.0	119.8(1)
C23—C21—H22	120.1	120.1
C19—C21—H22	119.9	120.1
C21—C23—C25	120.1	119.9(2)
C21—C23—H24	120.0	120.0
C25—C23—H24	120.0	120.0
C23—C25—C27	120.1	120.3(2)
C23—C25—H26	120.0	119.8
C27—C25—H26	119.9	119.8
C18—C27—C25	120.0	120.3(1)
C18—C27—H28	119.3	119.9
C25—C27—H28	120.7	119.9

4.2. HYDROGEN BONDING

In the crystal structure, three intermolecular N-H…O hydrogen bonds are observed. The N-H and NH_2 site of the creatininium cations are making strong hydrogen bonds with the carboxylate O atoms of the benzoate anions. In general, hydrogen bonds will cause a downshifting of stretching mode of vibrations and up shifting of deformation modes [30, 31]. This is reflected in the infrared and Raman spectra. This shifting is down around 120 cm^{-1} from the expected free ion value. Normally, the linear distortion is much greater than the angular distortion leading to the linear distortion shift as a high value. That is observed in the present case.

4.3. FACTOR GROUP ANALYSIS

The numbers of normal modes of creatininium benzoate crystals were determined by group theory analysis using the correlation method [32-34]. The results obtained are presented in Table 2. The total set of optic vibrations of creatininium benzoate crystal lattices are distributed as…..

$\Gamma = 90A_g^{IR,R} + 90B_g^{IR,R} + 89A_u^{IR} + 88B_u^{IR}$ excluding the $A_u^{IR} + 2B_u^{IR}$ species of acoustic modes. The A_g and B_g species are infrared and Raman active. Other two vibrational species A_u and B_u are infrared active only.

Table 2: Factor group analysis of creatininium benzoate $(C_4H_8N_3O)^+.(C_7H_5O_2)^-$, space group: $P2_1/c = C_{2h}$; $z^b = 4$

	Modes and degrees of freedom for each species		Site symmetry C_1	Factor group analysis C_{2h}
Creatininium $(C_4H_8N_3O)^+$	Vibrational	168	A	$42A_g+42B_g+42A_u+42B_u$
Benzoate $(C_7H_5O_2)^-$	Vibrational	144	A	$36A_g+36B_g+36A_u+36B_u$
	Translational	12	A	$3A_g+3B_g+3A_u+3B_u$
	Libration	12	A	$3A_g+3B_g+3A_u+3B_u$

$\Gamma_{\text{vibrational}} = 78A_g^{IR,R} + 78B_g^{IR,R} + 78A_u^{IR} + 78B_u^{IR}$; $\Gamma_{\text{translational}} = 3A_g^{IR,R} + 3B_g^{IR,R} + 3A_u^{IR} + 3B_u^{IR}$;

$\Gamma_{\text{rotational}} = 3A_g^{IR,R} + 3B_g^{IR,R} + 3A_u^{IR} + 3B_u^{IR}$;

$\Gamma_{crystal}^{total} = \Gamma_{(C_4H_8N_3O)^+} + \Gamma_{(C_7H_5O_2)^-} = 84A_g^{IR,R} + 84B_g^{IR,R} + 84A_u^{IR} + 84B_u^{IR}$; $\Gamma_{\text{acoustic}} = A_u^{IR} + 2B_u^{IR}$;

$\Gamma_{crystal}^{optical} = \Gamma_{crystal}^{total} - \Gamma_{acoustic} = 84A_g^{IR,R} + 84B_g^{IR,R} + 83A_u^{IR} + 82B_u^{IR}$

4.4. VIBRATIONAL ASSIGNMENTS

Creatininium benzoate crystal is in C_{2h} point group symmetry. The molecule has 30 atoms and 84 normal modes of fundamental vibrations, which is shown in the irreducible representations of factor group analysis and theoretical computation. The normal modes of vibrations are classified into skeletal and fingerprint vibrations that involve many of the atoms to move the same extent and characteristic group vibrations, which involve only a small portion of the molecule. The crystal creatininium benzoate is identified with many functional groups like, NH_2, NH, CH_3, CH_2, C=O, C-N, COO^-, C-OH, C-C=O, C-C-O and O-C-O. In addition skeletal vibrations like C-C, C-C-C, C-C-N, C-N-C, N-C-N and C-C-C-C are also exist in this compound. The characteristic wavenumbers of these groups are expected to change in their intensity and position according to their environment and the hydrogen bonding association in the crystal packing and are observed.

Infrared spectra of aromatic compounds contain characteristic bands between 4000 and 800 cm^{-1}. These bands are primarily associated with the motion of the benzene ring at the aromatic C-H bonds. The higher wave number region around 3500-1500 cm^{-1} consist the bands due to CH_3, CH_2, C=O, COO^-, C-N, N-H and C-H stretching vibrations. The lower wave number region around 1500 – 450 cm^{-1} contains bands due to deformation, twisting and rocking vibrations of the various groups. The skeletal vibrations are all coupled together and they occur in the region around 1150-500 cm^{-1}. The lattice vibrations occur below 400 cm^{-1}.

The observed wavenumbers, the calculated wavenumbers by DFT/B3LYP with 6-311++G(d,p) basis set method and the proposed assignments are given in Table 3. Comparison of these frequencies calculated at B3LYP with experimental values (Table 3) exposes the overestimation of the calculated vibrational modes due to the exclusion of anharmonicity in real system. Reduction in the computed harmonic vibrations, through basis set are only marginal as observed in the DFT values using 6-311++G(d,p). Apart from the level of calculations, it is customary to scale down the calculated harmonic frequencies in order to improve the agreement with the experiment.

Table 3 : The assignments of experimental wavenumbers, the calculated wavenumbers by using the DFT/B3LYP method with *311++G(d,p)* basic sets compared with the experimental wavenumbers for creatininium benzoate crystal

Mode numbers	Infrared $\bar{\nu}$ / cm^{-1}	Raman $\bar{\nu}$ / cm^{-1}	*B3LYP / 6-311++G(d,p)*	Assignment
1		3581 w	3563.8	N-H asym. stretching (NH_2)
2			3286.4	N-H asym. stretching (hydrogen bonded dimer)
3			3209.3	Aromatic CH asym. stretching
4			3201.6	Aromatic CH asym. stretching
5			3186	Aromatic CH asym. stretching
6			3175.6	Aromatic CH asym. stretching
7			3163.6	Aromatic CH asym. stretching
8	3107 br	3081 s	3114	CH_3 asym. stretching
9			3079.7	CH_3 asym. stretching + CH_2 asym. stretching
10			3069.1	CH_2 asym. stretching, CH_3 sym. stretching
11			3017	CH_2 sym. stretching
12	2973 br	2938 s	2997.6	CH_2 sym. Stretching, CH_3 sym. stretching
13		2815 w	2769.9	NH sym. stretching, N-H…O stretching, C-N asym. stretching
14	1807 sh	1801 w	1827.8	C=O stretching
15	1764 sh	1749 w	1730.4	C=O stretching, C-N asym. stretching
16	1718 vs	1690 w	1690.3	NH_2 scissoring, CN stretching, C=O stretching
17			1642	CH in plane bending, C-C stretching
18	1600 s	1601 vs	1620.8	CH_2 rocking, C=O stretching
19	1564 s	1573 sh	1529.6	C-N asym. stretching, COO^- asym. stretching
20	1523 s		1523.4	CH_3 asym. deformation, CH_2 scissoring
21			1516.7	COO^- asym . stretching, CH_3 sym. deformation
22			1503.2	CH_2 wagging, C-H in plane deformation
23		1487 w	1491.9	CH_2 twist
24			1478.8	CH_2 twist
25			1475.3	CH stretching
26			1453.2	CH stretching
27	1419 sh	1429 m	1425.2	C-O stretching, CH_3 asymmetric deformation
28	1381 vs	1381 s	1357.3	COO^- sym. stretching, CH_3 symmetric deformation
29			1348.3	C-C-N asym. stretching, CH_2 wagging
30		1330 w	1341.6	C-N sym. stretching
31			1320.1	C-N stretching
32	1298 w		1300.8	C-N sym. stretching, CH_2 wagging
33			1254.7	C-O stretching
34	1230 m		1235.5	Aromatic C-H Bending
35			1198.3	Aromatic C-H Bending
36		1190 w	1196.7	CH_2 rock
37	1172 w		1182.7	Aromatic C-H Bending
38		1154 w	1146.2	COO^- scissoring
39			1140.5	O-C=O in plane deformation
40	1121 m		1121	NH bending, C-C-N asym. stretching
41			1098.7	CH in plane bending
42			1061	OH out plane bending, C-C-N asym. stretching

43	1046 m		1045.7	Ring breathing, OH stretching
44			1040.2	CH_3 twisting
45		1023 m	1017.9	Ring breathing, CN symmetric stretching
46			1013.2	CH_2 twisting, C=O stretching, CN symmetric stretching
47		1004 vs	1011.8	C-C in plane bending, CH_3 rocking
48	998 w		1001.2	C-C stretching, CH bending
49	943 w		962.5	CH stretching
50	882 m	883 m	893.8	CH_2 bending, NH bending, C-C-N sym. stretching
51			865.5	CH bending
52			848.5	NH out plane bending
53	833 m	834 s	838.8	Ring breathing
54			829.2	CH out plane bending, C=O out plane bending
55			812.7	Ring deformation, OH stretching
56			728.5	C=N out plane bending
57	712 s	706 sh	724.3	C=O out plane bending
58	680 m		699.1	CH out plane bending
59			682.8	NH twisting
60			678.4	C=O in plane bending, CH stretching
61			674	NH stretching
62	649 m	651 m	632.3	C-C=C in plane bending, COO^- scissoring
63	598 w	596 s	599.8	O-C=O in plane deformation, NH in plane bending
64	571 m	572 m	578.8	CH_2 twisting, COO^- wagging
65		558 w	571.7	C-C=O in plane deformation
66		492 w	523.4	C-C in plane bending, COO^- rocking
67			448.7	C-C-C-C in phase deformation
68	418 w	419 w	416.5	C-C-C-C out phase deformation
69			414.4	C=O stretching, N-H bending, OH stretching
70		390 w	403.3	Ring breathing, OH stretching
71		315 w	313.7	Ring breathing
72			267.2	OH in plane bending
73		206 w	184.4	CH_2 twisting, NH_2 bending
74			174.8	CH_2 rocking, O-H stretching
75			157	C-NH_2 in plane bending
76			133.4	NH stretching
77		114 w	112.5	NH stretching
78		102 w	101.8	CH_3 wagging
79			99.5	CH_2 bending, CH_3 twisting
80			75.5	NH in plane bending
81			69.9	C=O bending
82			64.4	Lattice vibration
83			27.3	Lattice vibration
84			20.6	Lattice vibration

4.5. VIBRATION OF THE CREATININIUM CATION

The creatininium cation is linked to anion through three two centered N-H…O hydrogen bonds. This strong and moderate hydrogen bonds lead to downshifting of the stretching mode of vibrations in high wave

number region. The N-H asymmetric stretching frequency is observed at 3581 cm^{-1} in the Raman spectrum. The N-H asymmetric stretching (hydrogen bond dimer) is observed in theoretical calculations at 3286 cm^{-1} (mode 2) by DFT. As well, the amine group shows the bending vibrational wavenumbers in the regions of 1660-1610 cm^{-1}. The very strong band at 1718 cm^{-1} in infrared and weak band at 1690 cm^{-1} in Raman are assigned to the scissoring vibrational modes of NH_2 group. The theoretical calculations predict this wavenumber at 1690 cm^{-1} (mode 16). In IR spectrum, the wavenumber is found to be red shifted with Δ = 28 cm^{-1}. The position and intensity of the absorptions are disturbed due to the presence of hydrogen bonding. Since hydrogen bonding weakens in the N—H bond, stretching wavenumbers are downshifted and bending wavenumbers are upshifted [30, 31].

The C-N asymmetric stretching and symmetric stretching mode of vibration lies in the expected region. It is observed that weak peak at 2815 and 1330 cm^{-1} in the Raman spectrum corresponding to CN stretching [33, 35]. These vibrations are in good agreement with the theoretical assignment (mode 13 and mode 30) given by DFT. The medium peak at 1121 cm^{-1} in the Raman spectrum is attributed to the C-C-N asymmetric stretching vibration. The medium peak at 882 cm^{-1} in the Infrared spectrum and 883 cm^{-1} in the Raman spectrum is attributed to the C-C-N symmetric stretching vibration. Along with this vibration N-H bending mode also observed. These vibrations are also good agreement with the theoretical assignment (mode 40 and mode 50).

The CH_3 asymmetric and symmetric stretching modes are expected to occur at 2970 and 2880 cm^{-1}, respectively [32]. In this compound, the presence of Raman line at 3081 cm^{-1} and the infrared line at 3107 cm^{-1} correspond to the -CH_3 asymmetric stretching mode. The –CH_3 symmetric stretching mode is confirmed by the Raman band at 2938 cm^{-1} and the infrared line at 2973 cm^{-1}. Generally, the wavenumber of the CH_2 vibrational mode depends on its immediate environment. The -CH_2 stretching mode observed along with the –CH_3 stretching mode in the Infrared and Raman spectra. These –CH_3 & –CH_2 vibrations are predicted at 3114 and 2997.6 cm^{-1} from the theoretical assignment (mode 8 and mode 12), respectively. The medium intensity Raman line at 1429 cm^{-1} is due to CH_3 asymmetric deformation [32,35], which corresponds to a shoulder intensity line at 1419 cm^{-1} in the Infrared spectrum. This assignment is correlated with the theoretical calculation at mode 27. A strong band at 1381 cm^{-1} in both the spectrum is assigned to CH_3 symmetric deformation and COO^- symmetric stretching modes of the vibrations, it also correlated with the DFT (mode 28). The spectral lines in the region of 1000-1100 cm^{-1} are due to C-N symmetric stretching vibrations. In our case, the theoretically calculated value at 1017 cm^{-1} (mode 45) has a good agreement with the experimental values [36]. A strong band at 1004 cm^{-1} in Raman spectrum is due to the rocking mode of the CH_3 group vibration coupled with the C-C in-plane bending frequency. However, the theoretical calculations predict the wavenumber at 1011 cm^{-1} (mode 47) by DFT/B3LYP with 6-311++G(d,p) basis set.

The bending frequencies like wagging, rocking and twisting modes of CH_2 vibrations have been greatly influenced in the spectra [35, 36]. Generally, the wagging modes of CH_2 groups are expected to spread out over a wide frequency region, viz., 1382-1170 cm^{-1}. Here, the CH_2 wagging mode is observed as a weak band at 1298 cm^{-1} in Infrared spectrum. The rocking frequencies of the CH_2 group are observed at a weak line 1190 cm^{-1} in Raman spectrum. Weak bands at 206 cm^{-1} in Raman spectrum is due to the CH_2 twisting mode of vibration. These values are good in agreement with the theoretical calculations predicts the mode 32, mode 36 and mode 73, respectively. These assignments agree well with the values available in the literature [32, 33, 35, 36].

4.6. VIBRATION OF THE BENZOATE ANION

The ionized carboxylic group gives rise to COO^- asymmetric stretching observed as a strong peak at 1564 cm^{-1} in Infrared spectrum and a shoulder peak at 1573 cm^{-1} in Raman spectrum [33]. The theoretical calculations predict the band at 1529 cm^{-1} (mode 19). Already, COO^- symmetric stretching discussed in detail with the CH_3 symmetric deformation. The COO^- bands are altered than the expected range to strong hydrogen bonding interactions as observed in XRD.

The rocking, wagging and scissoring in-plane and out-of-plane deformation modes of COO^- ionized carboxylic group are expected at 502, 577 and 665 cm^{-1}, respectively [32, 33]. For the title compound, the rocking mode occurs at 492 cm^{-1} in Raman and the wagging mode appears at 571 cm^{-1} in IR spectrum and 572 cm^{-1} in Raman spectrum. The scissoring deformation mode is identified as medium intensity lines at 649 cm^{-1}

in IR spectrum and 651 cm^{-1} in Raman spectrum. These modes are in good agreement with the theoretical calculations by DFT (mode 66, mode 64 and mode 62, respectively).

The O-C=O in-plane deformation mode is observed as a strong intensity line at 596 cm^{-1} in Raman spectrum and a weak line at 598 cm^{-1} in Infrared spectrum. In our case, the theoretically calculated value at 599 cm^{-1} (mode 63) has a good agreement with the experimental values [36].

Normally, the absorption bands in the region 3600 - 3200 and 3100 - 3000 cm^{-1} are due to O-H and C-H stretching vibrational modes of phenol. The C-C-C-C in-phase deformation modes are observed at 448 cm^{-1} in theoretical calculation (mode 67). The out-of-phase deformation modes are observed as a weak peak at 416 cm^{-1} in Raman spectrum and 418 cm^{-1} in Infrared spectrum. The theoretical calculations predict the wavenumber at 416 cm^{-1} (mode 68).

5. CONCLUSION

The recorded FT-IR and FT-Raman spectra and the detailed vibrational assignment were presented. The equilibrium geometries with the harmonic frequencies of creatininium benzoate were determined and analyzed by DFT B3LYP/6-311++G(d,p) level of theory. The H atom of the amine group in creatininium makes a hydrogen bond with a carboxyl group. On the basis of agreement between the calculated and observed results, assignments of fundamental vibrational modes of creatininium benzoate were examined and slight difference between the observed and scaled wavenumber is identified and discussed. This noted discrepancy may be due to the fact that the calculations have been actually done on a single molecule in the gaseous state, but the experimental values are recorded in the solid phase where the intermolecular interactions are playing major role in stabilizing the structure. Therefore, the assignments made by DFT B3LYP/6-311++G(d,p) level of theory matches with the experimental values, confirms the molecular structure of creatininium benzoate.

REFERENCES

1. Madaras M.B and Buck R.P., Anal. Chem. 1996, 68, 3832.
2. Butler A.R. and Glidewell C.J., J. Chem. Soc. Perkin Trans.,1985, 2, 1465.
3. Kotsyubynskyy D., Molchanov S. and Gryff-Keller A., Pol. J. Chem. 2004,78, 239.
4. Craw J.S., Greatbanks S.P., Hillier I.H., Harrison M.J. and Burton N.A., J. Chem. Phys. 1997, 106, 6612.
5. Reddick R.E. and Kenyon G.L., J. Am. Chem. Soc., 1987, 109, 4380.
6. Olofson A., Yakushijin K. and Horne D.A., J. Org. Chem., 1998, 63, 5787.
7. Canty A.J., Fyfe M., Gatehouse B.M., Inorg. Chem., 1978, 17, 1467.
8. Udupa M.R. and Krebs B., Inorg. Chim. Acta, 1979, 33, 241.
9. Muralidharan S., Nagaraja K.S. and Udupa M.R., Transit. Met. Chem., 1984, 9, 218.
10. Okabe N., Kohyama Y. and Ikeda K., Acta Cryst., 1995, C51, 222.
11. Celal Bayrak, Sevgi Haman Bayari, Hacettepe, J. Biol. & Chem., 2010, 38, 107.
12. Benali-Cherif N., Bendheif L., Bouchouit K. and Cherouana A., Ann. Chim. Sci. Mater., 2004, 29, 11.
13. Bouchouit K., Benali-Cherif N., Benguedouar L., Bendheif L. and Merazig H., Acta Cryst., 2002, E58, o1397.
14. Bendheif L., Benali-Cherif N., Benguedouar L., Bouchouit K. and Merazig H., Acta Cryst., 2003, E59, o141.
15. Kagan C.R., Mitzi D.B. and Dimitrakopoulos C.D., Science, 1999, 286, 945.
16. Richards M.F., Wyckoff H.W., Carison W.D., Allewell N.M., Lee M. and Mitsui Y., Cold Spring Harbor Symp. Quant. Biol., 1972, 36, 25.
17. Pesrutz M.F. and Ten Eyck I.F.. Cold Spring Harbor Symp. Quant. Biol. 1972, 36, 295.
18. Berrah F., Lamraoui H. and Benali-Cherif N., Acta Cryst., 2005, E61, o210.
19. Bahadur S.A., Sivapragasam S., Kannan R.S. and Sridhar B., Acta Cryst., 2007, E63, o1714.
20. Moghimi A., Sharif M.A. and Aghabozorg H., Acta Cryst., 2004, E60, o1790.
21. Frisch M.J., Trucks G.W., Schlegel H.B., Scuseria G.E., Robb M.A., Cheeseman J.R., Montgomery J.A., Jr., Vreven T.,. Kudin K.N, Burant J.C., Scalmani G., Raga N., Peterson G.A., Nakasuji H., Hada M., Ehara M., Toyota K., Fukuda R., Hasegawa J., Ishida M., Nakajima T., Honda Y., Kitao O., Nakai H., Klene M.,. Li X, Knox J.E., Hratchian H.P., Cross J.B., Adamo C., Jarmaillo J., Gomperts R., Stratmann R.E., Yazyev O., Ustin A.J., Cammi R., Pomelli C., Ochterski J.W., Ayala P.Y., Morokuma K., Salvador

V.P., Dannenberg J.J., Zakrzewski V.G., Dapprich S., Daniels D., Strain M.C., Farkas O., Malick D.K., Rabuck A.D., Raghavachari K., Foresman J.B., Ortiz J.V., Cui Q., Baboul A.G., Clifford S., Cioslowski J., Stenfanov B.B., Liu G., Liashenko A., Piskorz P., Omaromi I., Martin L., Fox D.J., Keith T., Al-Laham M.A., Peng C.Y., Anayakkara, Challacombe M., Gill P.M.W., Johnson B., Chen W., Wong M., Gonzalez C., and Pople J.A., Gaussian Inc., Wallingford CT, 2004.

22. Schlegel H.B., J. Comput. Chem., 1982, 3, 214.
23. Hohenberg P. and Kohn W., Phys. Rev., 1964, 136, B864.
24. Becke A.D., J. Chem. Phys., 1993, 98, 1372; Becke A.D., J. Chem. Phys., 1993, 98 5648.
25. Lee C., Yang W. and Parr R.G., Phys. Rev., 1988, B37, 785.
26. Frisch A., Nielson A.B. and Holder A.J., GAUSSVIEW User Manual, Gaussian Inc., Pittusburgh, PA, 2000.
27. Tariq M.I., Ahmad S., Tahir M.N., Sarfaraz M. and Hussain I., Acta Cryst., 2010, E66, o1561.
28. Smith G., and White J.M., Aust. J. Chem., 2001, 54, 97.
29. Majerz I., Sawka-Dobrowolska W. and Sobczyk L., Journal of Mol. Struc., 1993, 297,177.
30. Aruldhas G., Molecular Structure and spectroscopy, 2001, Prentice Hall of India, New Delhi,.
31. Brown I.D., Acta Cryst., 1976, A32 24.
32. F. Albert Cotton, Chemical Applications of Group Theory, 1990, 3rd ed. John Wiley & Sons, Singapore,.
33. Fateley W.G., Dollish F.R., McDevitt N.T. and Bentley F.F., Infrared and Raman Selection Rules for Molecular and Lattice Vibrations, 1972, Wiley, New York, NY,.
34. Colthup N.B., Daly L.H. and Wiberley S.E., Introduction to Infrared and Raman Spectroscopy, 1990,Academic Press, New York, NY,.
35. John Coates, Encyclopedia of Analytical Chemistry, R.A. Meyers (Ed.), John Wiley& Sons Ltd, USA.
36. Dollish F.R. and Fateley W.G., Characteristic Raman Frequencies of Organic-Compounds, 1973,Wiley, New York.

*****